PHYSICAL REVIEW B VOLUME 58, NUMBER 6 1 AUGUST 1998-II

First-order spin-paramagnetic transition and tricritical point in ultrathin Be films

P. W. Adams and P. Herron
Department of Physics and Astronomy, Louisiana State University, Baton Rouge, Louisiana 70803

E. I. Meletis
Department of Mechanical Engineering, Materials Science and Engineering Program, Louisiana State University, Baton Rouge, Louisiana 70803

(Received 12 January 1998)

We report measurements of the parallel critical magnetic field of thin superconducting beryllium films with $T_c \sim 0.6$ K. The critical field transitions were spin-paramagnetically limited and found to be strongly hysteretic below a tricritical point at $T_{\rm tri} = 190$ mK. The magnitude of the hysteresis and $T_{\rm tri}$ were observed to be completely suppressed in field misalignments $\theta \geqslant 1°$. Time relaxation measurements in the hysteretic regime showed simple exponential decays in the highest quality films and nonexponential decays interspersed with avalanches in more inhomogeneous samples. [S0163-1829(98)51030-2]

The parallel critical magnetic-field behavior of thin-film superconductors has garnered a great deal of theoretical and experimental interest over the past 30 years.[1,2] In sufficiently thin films the orbital currents are suppressed and the coupling of the field to the electronic spins drives the system into the normal state in what is commonly known as the spin paramagnetic transition.[1] Much of the interest in this transition can be traced back to the pioneering theoretical work of Clogston and Chandrasekhar,[3] which predicted that a parallel field, $H_\parallel$, would limit thin-film superconductivity by way of a first-order transition when the Zeeman splitting of the quasiparticles was equal to the superconducting condensate energy. In terms of the transition temperature, T_c, the transition occurs at a critical field $H_{c\parallel} \sim (1.86\ T/K) T_c$.[2] In practice, $H_{c\parallel}$ can be more than an order of magnitude greater than the perpendicular critical field, H_{c2}.[4] A more in-depth analysis of the spin paramagnetic transition showed it would be of first order only in systems with a sufficiently low spin orbit scattering rate, $1/\tau_{\rm so}$; otherwise the transition is second order.[1] In the limit of $1/\tau_{\rm so} = 0$ the transition was predicted to go from second order to first order at a tricritical point $T_{\rm tri} \sim 0.6 T_c$.[5] Early experiments on thin, superconducting, granular Al films with transition temperatures $T_c \sim 2$ K suggested that in Al $T_{\rm tri} = 0.34 T_c$.[6] However, these measurements were only carried down to 400 mK, and no significant hysteresis in $H_{c\parallel}$ was ever found to substantiate a first-order transition.

Recently, parallel magnetic-field studies of granular Al films were extended to lower temperatures and a giant hysteresis was found in the parallel critical field $H_{c\parallel}$ below 270 mK.[7,8] This work conclusively demonstrated a tricritical point at $T_{\rm tri} \sim 270$ mK in Al ($T_{\rm tri} \sim 0.15 T_c$), independent of film sheet resistance.[8] This discovery offered a unique opportunity to study the dynamics of the Al films in the hysteretic regime where they could be brought far out of thermodynamic equilibrium.[9] The results of these experiments revealed some rather unusual behavior. Relaxation to equilibrium in fields just below $H_{c\parallel}$ was observed to occur via very slow, glasslike, stretched-exponential relaxations interspersed with numerous avalanches. A statistical analysis of the avalanche behavior revealed a power-law size distribution $D(s) \sim s^{-2}$.[9] Furthermore, angular studies of the hysteresis showed an exponential decrease in its magnitude with increasing field misalignment.[8] The characteristic angle of this dependence was $\theta_c = 2.4°$. These observations raised several important unanswered questions about the origin of the critical field hysteresis and its associated glasslike dynamics.

In particular, it is still not known what role microscopic film morphology plays in the nonequilibrium behavior. Aluminum films are highly granular[10] and global superconductivity in these films is mediated by intergrain Josephson coupling.[7,11] High resistance granular Al films also show clear evidence of grain charging effects.[7,12] Since Josephson coupling and grain charge quantization are incompatible,[13] the anomalous dynamics of Al films may result from competition between these two phenomena. Furthermore, a first-order spin paramagnetic transition has never been conclusively found in any material other than Al. To see tricritical point behavior in another system would eliminate the possibility that Al is pathological in parallel field and would provide an important test of theory.[1,14] In this paper we present an investigation of the spin paramagnetic transition in thin, nongranular beryllium films with $T_c \sim 0.6$ K. We have discovered a first-order spin paramagnetic transition and a tricritical point at $T_{\rm tri} = 190$ mK. Angular studies of the critical field hysteresis reveal that Be films are six times more sensitive to field alignment than Al films.[8] Furthermore, in contrast to the glassy behavior of granular Al films in the hysteretic region,[9] the time dependence of our most homogeneous Be films are exponential in character with a decay rate that is a strong function of $|H_{c\parallel} - H_\parallel|$. Our results suggest that film morphology plays an important role in determining the dynamics of the nonequilibrium state.

The Be films used in this study were made by thermally evaporating 99.5% pure beryllium powder onto fire-polished glass substrates held at 84 K. The evaporations were made in a 4×10^{-7} Torr vacuum at a rate ~ 0.10 nm/s. The film area was 1.5 mm$\times$4.5 mm. The resistance of the Be films was measured during the evaporation. Typically, electrical conti-

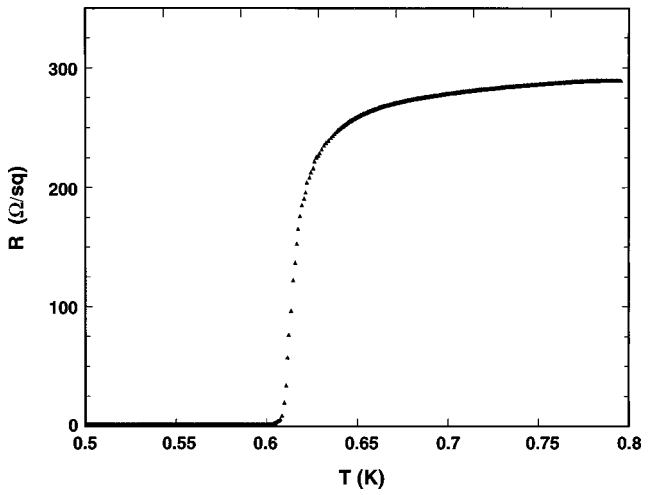

FIG. 1. Superconducting transition for a 4.2 nm nominally thick Be film in zero magnetic field.

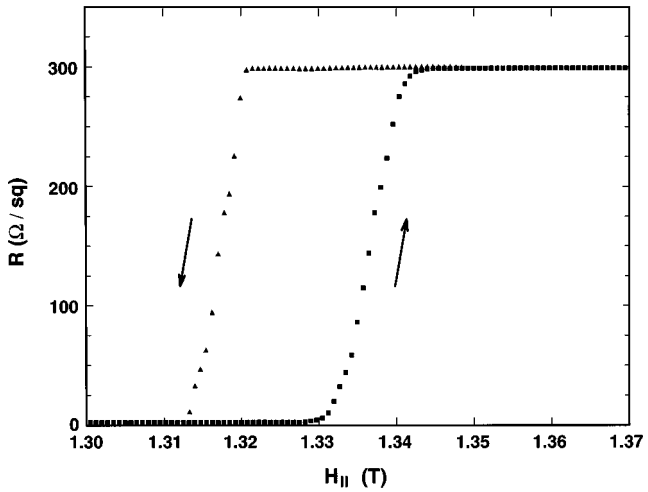

FIG. 2. Parallel critical magnetic-field transition at 30 mK showing hysteresis. The arrows depict the field sweep direction. The field sweep rate was 0.25 G/s.

nuity was observed at a film thickness $d \sim 1$ nm.[15] This exceedingly low threshold for continuity reflects the fact that the Be formed astonishingly uniform films on fire-polished glass. Scanning force micrographs of the films' exposed oxide surface did not reveal any salient morphological features down to the 0.7 nm scale. In fact, the films seemed to be as ''smooth'' as the fire-polished glass on which they were deposited. In addition, analytical transmission electron microscopy was used for microstructural analysis of 15-nm-thick Be films deposited on cleaved NaCl crystals at 84 K. High magnification (250,000×) micrographs revealed that the films were composed of an ultrafine base structure that was interspersed with 5–15 nm Be nanocrystallites. Electron diffraction studies showed no diffraction from the metallic base structure suggesting that it was amorphous. Similarly the oxide (BeO) produced a broad, continuous diffraction ring indicating its grain size was <1 nm.[16]

For the purposes of the present study, films with thicknesses of ~ 4.0 nm and normal state sheet resistances $R_n = 300-500\ \Omega/\mathrm{sq}$ proved to be ideal. Significantly thicker films showed a depressed tricritical point due to finite thickness effects and thinner films with $R_n > 1\ \mathrm{k}\Omega/\mathrm{sq}$ had significantly lower T_c's (i.e., $T_c \sim 65$ mK for a film with $R_n \sim 5\ \mathrm{k}\Omega/\mathrm{sq}$). After the evaporation, the bell jar was opened and the Be films were exposed to air. A surface oxide layer subsequently formed on the film's surface. The thickness of Be consumed by the oxidation was found to be 1.0–1.5 nm as measured by a transient upward drift in both the crystal thickness monitor reading and R_n. We also exposed the films to 1 atm of ultrapure O_2 and found no significant difference in the final oxide thickness. We believe that the oxide layer was a self-limiting barrier type.[17] Four-wire resistances were measured with probe currents of 50 nA using a lock-in amplifier operating at 27 Hz. The samples were cooled down to 30 mK using a dilution refrigerator operating in magnetic fields up to 9 T. Film orientation to the applied field was controlled with 0.1° resolution by an *in situ* mechanical rotator.

Shown in Fig. 1 is sheet resistance versus temperature in zero field for a Be film with a normal-state resistance of $R_n = 300\ \Omega/\mathrm{sq}$ and a $T_c = 0.62$ K. The nominal thickness of the film was 4.2 nm. The actual metallic thickness was ~ 3.0 nm after oxidation in air. From measurements of dH_{c2}/dT at T_c,[18] we calculated a mean-free path of $l_0 = 64$ nm and a coherence length $\xi_0 = 56$ nm for the film in Fig. 1. Though bulk Be has a very low $T_c^{\mathrm{bulk}} \sim 26$ mK, it has been known since the late 1950's that quenched condensed Be films (i.e., films evaporated onto liquid helium cooled substrates) have surprisingly high transition temperatures.[19] In fact, quenched condensed Be has the highest elemental transition temperature $T_c \sim 9\ \mathrm{K} \sim 400 T_c^{\mathrm{bulk}}$. Unfortunately, warming a quenched condensed Be film to room temperature causes an irreversible structural transition and the high transition temperature is lost.[20] Nevertheless, Fig. 1 demonstrates that between fabrication and measurement[21] thin Be films can be handled in air and still have $T_c > 10 T_c^{\mathrm{bulk}}$.

In Fig. 2 we show the parallel critical field transition at 30 mK for the film in Fig. 1. The field was swept at a rate of

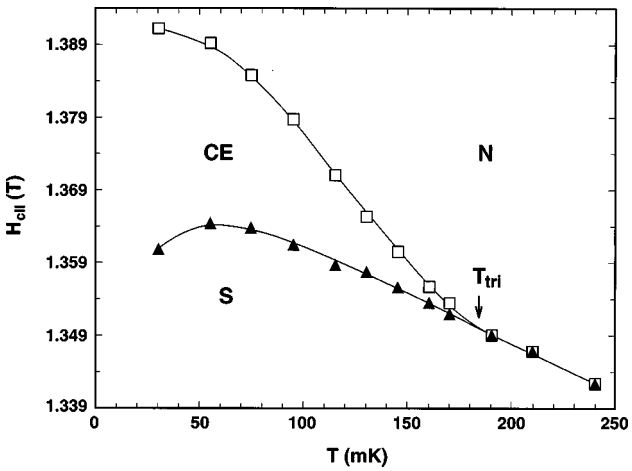

FIG. 3. Parallel critical fields versus temperature measured from field sweeps at fixed temperatures for a film with $R_n = 310\ \Omega/\mathrm{sq}$. The squares depict up-sweep transitions and the triangles are down-sweep transitions. The solid lines are a guide to the eye. *S*: superconducting phase; *N*: normal phase; *CE*: coexistence region. The arrow indicates the tricritical point.

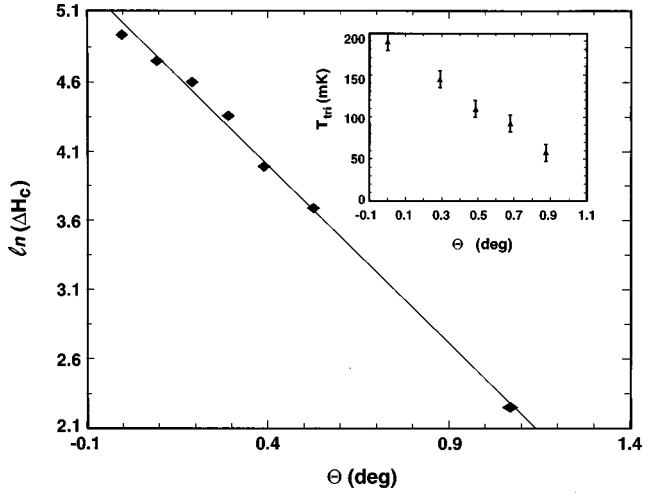

FIG. 4. Semilog plot of the hysteresis width as a function of field angle θ (parallel orientation corresponds to $\theta=0$) at 30 mK. The line is a least-squares fit to the data and gives a characteristic angle of $\theta_c=0.4°$. Inset: Tricritical point as a function of angle.

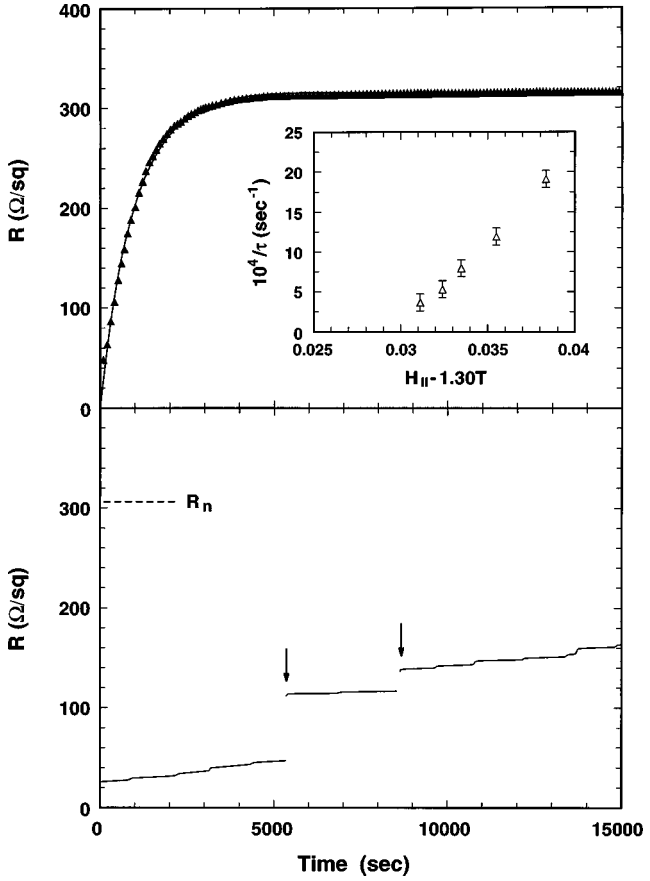

FIG. 5. Top: Time relaxation of sample No. 14B after sweeping the field up to the point where $R\sim 0.1R_n$. The solid line is a least-squares fit to the data using an exponential form. Inset: Relaxation rates of sample No. 14B at variety of fields in the hysteretic region. Bottom: Time relaxation of sample No. 14A after sweeping the field up to the point where $R\sim 0.1R_n$. The arrows point to avalanches. Samples No. 14A and No. 14B were fabricated simultaneously.

0.25 G/s in the directions depicted by the arrows in the figure. The values of the critical fields $H_{c\|}\approx 1.3$ T are in reasonable agreement with the Clogston limit of $H_{c\|}=(1.86\ \mathrm{T/K})T_c=1.15$ T and are more than an order of magnitude greater than the perpendicular critical field, $H_{c2}=0.106$ T. Note the large hysteresis in $H_{c\|}$ and the extraordinary sharpness of the transitions. The transitions are, in fact, approximately 0.5% wide as measured from 10% to 90% of the normal-state resistance. In comparison, the transitions in Al films are about 4% wide.[7] This difference probably reflects the unusually high degree of homogeneity of the films. The hysteresis shown in Fig. 2 was extremely sensitive to the field alignment. Parallel alignment was, in fact, achieved by varying the sample angle in order to maximize the magnitude of the low-temperature hysteresis (see discussion below). This technique enabled us to find parallel alignment to within 0.1°.

Shown in Fig. 3 are the parallel critical fields as a function of temperature for a film with $R_n=310\ \Omega/\mathrm{sq}$. The triangles represent the down-sweep midpoint critical fields and the squares are the up-sweep critical fields. At the lowest temperature the hysteresis is about 300 G. We believe that this indicates unambiguously that the spin paramagnetic transition is first order. As the temperature is raised, the first-order transition gives way to a second-order transition, as evidenced by the disappearance of hysteresis above a tricritical point at $T_{\mathrm{tri}}=190$ mK. Thus Fig. 3 can be interpreted as a phase diagram, where *S* represents the superconducting phase, *N* the normal phase, and *CE* a coexistence phase whose microscopic nature is still poorly understood. Though the T_{tri} is lower than that of Al ($T_{\mathrm{tri}}=270$ mK), the first-order transition is actually more robust in Be than Al. In Be films $T_{\mathrm{tri}}/T_c=0.33$, but in Al films $T_{\mathrm{tri}}/T_c=0.15$. This is almost certainly due to the lower atomic mass of Be resulting in a smaller spin-orbit scattering rate than that of Al.[22] However, the Be ratio is still a factor of 2 below the theoretical value $T_{\mathrm{tri}}/T_c=0.6$.[5]

In order to further probe the phase diagram shown in Fig. 3 we made extensive measurements of the angular dependence of the low-temperature hysteresis. In Fig. 4 we present a semilog plot of the magnitude of the hysteresis, ΔH_c, which is defined as the difference in the up-sweep and down-sweep critical fields, as a function of the angle of the film relative to the magnetic field θ. Parallel orientation corresponds to $\theta=0°$. Note the exquisite sensitivity of the hysteresis to angle. Misalignments greater than about 1° were enough to completely wash out the first-order transition. The linear behavior in Fig. 4 suggests an exponential dependence, $\Delta H_c(\theta)=\Delta H_c(0)\exp(-\theta/\theta_c)$. The solid line is a least-squares fit which gives a characteristic angle $\theta_c=0.4°$. Aluminum films have a similar angular dependence but with a much larger characteristic angle $\theta_c=2.4°$.[8] It is uncertain whether this difference is due to an intrinsic elemental property of the films or to the differing morphologies of Be and Al films. For instance, the granular Al films in Ref. 7 were nominally 5 nm thick in contrast to the ~1.5 nm metallic thickness of the Be films used in this study. In the inset of Fig. 4 we show the angular dependence of T_{tri}. Tilting the field not only suppresses the magnitude of the hysteresis but also the tricritical point. To date there is no theoretical description of these angular dependencies.

Finally, we investigated the dynamics of the films in the

hysteretic region. This was done by monitoring the film resistance R, while ramping the field up to a point just below $H_{c\|}$ at a rate of 1–2 G/s. The field sweep was stopped and the magnet put into persistent mode when a selected fraction of the normal-state resistance appeared in the sample. We then monitored R as a function of time as the film relaxed to thermodynamic equilibrium. Shown in the upper portion of Fig. 5 is such a time relaxation for the sample in Fig. 2 (No. 14B). The solid line is an exponential fit to the data, assuming the decay begins from the value of R at the time the field sweep was stopped, $R_0 \sim 50\ \Omega$/sq. The decay rate was very sensitive to the field, as can be seen in the inset of Fig. 5. Presumably the zero rate intercept of this plot represents the thermodynamic critical field.

In similar experiments on granular Al films the time dependence of R was always stretched exponential in form [i.e., $R(t) \sim \exp(\sqrt{t})$] with large numbers of avalanches superimposed on the relaxation curves.[9] Interestingly, the time dependence of some of our uniform Be films behaved similarly, for reasons that are not completely evident. For example, the data in the bottom portion of Fig. 5 (sample No. 14A) have a much slower relaxation rate, though R_0, R_n, and $T_{\rm tri}$ for this sample were about the same as those of sample No. 14B. Furthermore, the relaxation is dominated by the large avalanches as indicated by the arrows. Curiously, the two samples, No. 14A and No. 14B, in Fig. 5, were fabricated simultaneously. The parallel critical field transitions of No. 14B were extremely sharp (see Fig. 2), and perhaps this is why this particular film decayed exponentially. The parallel critical field transitions of sample No. 14A, which we have not shown, were twice as broad as those of No. 14B. We saw a similar correlation in other samples, which suggests that the avalanches and nonexponential decay were a result of film inhomogeneities and/or disorder. We believe that by sweeping the field up to a point where R_0 is finite, we are, in fact, nucleating normal phase regions in the film. Clearly, these regions must be of sufficient size and density to preclude a percolating zero resistance path along the direction of current flow. After the field sweep is halted, the size of the normal regions grows with time. Thus the relaxations in Fig. 5 represent the dynamics of the phase boundary between the normal and superconducting regions. Perhaps the pinning of these phase boundaries on defects and inhomogeneities is responsible for the behavior we see in the lower portion of Fig. 5.

In conclusion, we observe a robust first-order spin paramagnetic transition in Be films quenched condensed at 84 K. Measurements of the dynamics in the hysteretic regime show that Be films may relax via simple exponential decay or more complex decays involving nonexponential time dependence and avalanches. The fact that exponential decays are seen in many Be films but never seen in granular Al films suggests that the avalanche behavior is a consequence of phase boundary pinning. Future experiments in which decays are measured in high quality Be films that have been systematically disordered via irradiation should prove interesting.

We thank Dana Browne, John DiTusa, Wenhao Wu, and Kevin Bassler for many valuable discussions. We are grateful to Robin McCarley for the scanning force microscopy characterizations. This work was supported by NSF Grant Nos. DMR 9501160 and DMR 9204206.

[1] P. Fulde, Adv. Phys. **22**, 667 (1973).

[2] M. Tinkam, *Introduction to Superconductivity* (Krieger, Malabar, FL, 1980).

[3] A. M. Clogston, Phys. Rev. Lett. **9**, 266 (1962); B. S. Chandrasekhar, Appl. Phys. Lett. **1**, 7 (1962).

[4] Koya Aoi, R. Meservey, and P. M. Tedrow, Phys. Rev. B **9**, 875 (1974.).

[5] G. Sarma, J. Phys. Chem. Solids **24**, 1029 (1963); K. Maki and T. Tsuneto, Prog. Theor. Phys. **31**, 945 (1964); K. Maki, *ibid.* **32**, 29 (1964).

[6] P. M. Tedrow, R. Meservey, and B. B. Schwartz, Phys. Rev. Lett. **24**, 1004 (1970).

[7] Wehnao Wu and P. W. Adams, Phys. Rev. Lett. **73**, 1412 (1994).

[8] Wenhao Wu, R. G. Goodrich, and P. W. Adams, Phys. Rev. B **51**, 1378 (1995).

[9] Wenhao Wu and P. W. Adams, Phys. Rev. Lett. **74**, 610 (1995); P. W. Adams and Wenhao Wu, Physica B **210**, 479 (1995).

[10] Wenhao Wu, P. W. Adams, R. L. McCarley, and D. J. Dunaway, Appl. Phys. Lett. **65**, 1180 (1994).

[11] B. G. Orr, H. M. Jaeger, and A. M. Goldman, Phys. Rev. B **32**, 7586 (1985); A. E. White, R. C. Dynes, and J. P. Garno, *ibid.* **33**, 3549 (1986); D. B. Haviland, H. M. Jaeger, B. G. Orr, and A. M. Goldman, *ibid.* **40**, 719 (1989).

[12] Wenhao Wu and P. W. Adams, Phys. Rev. B **50**, 13 065 (1994).

[13] B. Abeles, Phys. Rev. B **15**, 2828 (1977).

[14] S. Frota-Pessôa and B. B. Schwartz, Solid State Commun. **20**, 505 (1976).

[15] Though electrical continuity in vacuum was achieved at $d \sim 1$ nm, films this thin quickly became discontinuous upon exposure to air. Films with $d > 2.0$ nm were stable in air after an initial transient.

[16] More details of the film's morphology will be published elsewhere.

[17] Minoru Okamoto, Koji Takei, Yasushi Maeda, and Masaru Igarashi, J. Appl. Phys. **59**, 2988 (1986); S. Sako, K. Ohshima, and T. Fujita, J. Phys. Soc. Jpn. **59**, 662 (1990).

[18] E. Hefland and N. R. Werthhamer, Phys. Rev. **147**, 288 (1966).

[19] B. G. Lazarev, A. I. Sudovtsov, and A. P. Smirnov, Zh. Eksp. Teor. Fiz. **33**, 1059 (1957) [Sov. Phys. JETP **6**, 816 (1958)]; R. E. Glover III, S. Moser, and F. Baumann, J. Low Temp. Phys. **5**, 519 (1971).

[20] C. G. Granqvist and T. Claeson, Z. Phys. B **20**, 13 (1975).

[21] Be films with $T_c \sim 6$ K can be grown at room temperature via ion sputtering; see K. Takei, K. Nakamura, and Y. Maeda, J. Appl. Phys. **57**, 5093 (1985).

[22] P. M. Tedrow and R. Meservey, Phys. Lett. **58A**, 237 (1976).